Astronomy & Astrophysics manuscript no.
(will be inserted by hand later)

The visible environment of galaxies with counterrotation

D. Bettoni[1], G. Galletta[2], and F. Prada[3]

[1] Osservatorio Astronomico di Padova, Vicolo dell'Osservatorio 5, 35122 Padova, Italy
[2] Dipartimento di Astronomia, Università di Padova, Vicolo dell'Osservatorio 2, 35122 Padova, Italy
[3] Centro Astronómico Hispano-Alemán, Apartado 511, E-04080 Almería, Spain

Received 6 February 2001; accepted 23 April 2001

Abstract. In this paper we present a statistical study of the environments of 49 galaxies in which there is gas- or stellar- counterrotation. The number of possible companions in the field (to apparent magnitude 22), their size and concentration were considered. All the statistical parameters were analysed by means of Kolgomorov-Smirnov tests, using a control sample of 43 galaxies without counterrotation. From our data, no significant differences between the counter-rotating and control samples appear. This is different to Seyfert or radio-loud galaxies which lie in environments with a higher density of companions. On the contrary, if a weak tendency exists, for galaxies with gas counterrotation only, it is discovered in regions of space where the large scale density of galaxies is smaller.
Our results tend to disprove the hypothesis that counterrotation and polar rings derive from a recent interaction with a small satellite or a galaxy of similar size. To a first approximation, they seem to follow the idea that all galaxies are born through a merger process of smaller objects occurring very early in their life, or that they derive from a continuous, non-traumatic infall of gas that formed stars later. Whatever the special machinery is which produces counterrotation or polar rings instead of a co-planar, co-rotating distribution of gas and stars, it seems not to be connected to the present galaxy density of their environments.

Key words. galaxies: evolution — galaxies: formation — galaxies: interactions — galaxies: peculiar

1. Introduction

In a previous paper (Brocca *et al.* 1997, Paper I) we studied the environment of galaxies circled by a polar ring of gas and stars, a kind of stellar system whose origin is still under discussion: in recent theoretical works the polar rings are obtained by means of a merging of galaxies (Bekki 1998), whereas in other studies, it is ascribed either to the accretion of matter during a close encounter with a nearby donor galaxy (Reshetnikov & Sotnikova 1997), or to the capture of gas or stars from the environment (Whitmore et al. 1990; Tremaine & Yu 2000). It is evident that in the three suggested scenarios, the present environment of these galaxies should appear different in the richness of small satellites or bright companions. For instance, in the hypothesis of a close encounter, the donor galaxy should not be too far from the polar ring galaxy, whereas in the case of diffuse gas, no visible differences are expected. The epoch of the 'second event' may also play a role in the possibility of detecting the donor galaxy. From the data of Paper I, we concluded that the environment of polar ring galaxies appears to be similar to that of normal galaxies in relation to the richness, density or concentration of satellites. We deduced that this result favours the infall of matter or a very early merger theory.

A different result has been found by analysing the environment of other galaxy categories, whose peculiar origin has been connected in the literature to galactic interactions or mergers (Gunn 1979), similar to polar rings. In particular, the environment of Seyfert galaxies appears to be richer in physical companions than that of normal galaxies (Dahari 1984; Rafanelli *et al.* 1995). Similarly, the local galaxy density of 47 radio-loud elliptical and lenticular galaxies appears higher than that of radio-quiet galaxies by a factor 2-3 (Heckman *et al.* 1985). Even radio-loud QSO with $0.9<z<1.5$ appear surrounded by a statistically significant excess of galaxies (Hintzen *et al.* 1991). Among these peculiar environments, the apparent normality of polar ring galaxies looks anomalous and distinguishes them from the other categories of astronomical objects whose peculiarity or activity is ascribed to interaction or merger. Therefore, we wish to see if other types of peculiar galaxies have an environment similar to that of the active galaxies or if they are 'normal' in this respect, as the polar ring galaxies appear to be.

In this paper, the environment of another category of peculiar galaxies, in which the rotation of the gas or of the

Send offprint requests to: G. Galletta

stars is opposite to that of most of the stars in the galaxy, is analysed. This phenomenon, known as 'counterrotation', presents a variety of aspects: it may be present in the gas only (Bettoni 1984; Caldwell *et al.* 1986; Galletta 1987; Ciri *et al.* 1995), in a portion of the stars (Bender 1988; Franx 1988; Jedrzejewski & Schecther 1988; Bettoni 1989; Rubin *et al.* 1992; Merrifield and Kuijken 1994; Prada *et al.* 1996, 1999) or in both (Bertola *et al.* 1996; Galletta 1987). The existing observations suggest that counterrotation is a phenomenon which is present all along the Hubble sequence. As in the case of polar ring galaxies, the origin of the counterrotation has been attributed to different mechanisms. One of these is the collision between the accretor galaxy and a small satellite (Kennicut 1996; Thakar and Ryden 1996). The difference to the formation of a polar ring may reside in the satellite orbit, coplanar with the disk of the accretor (and retrograde) to generate counterrotation (Thakar and Ryden 1996). Another mechanism may be the merger of two spirals of unequal mass (Balcells & Gonzalez 1998; Bekki 1998), which is able to transfer matter as large as 10^8 $M_\odot$ or more in counterrotation (Bettoni *et al.* 1991; Rubin *et al.* 1992; Ciri *et al.* 1995; Bettoni *et al.* 1999). A third alternative involves an extended period of star- or gas- infall during which the spin of the accreted matter changes rapidly (Voglis *et al.* 1991; Quinn & Binney 1992; Merrifield and Kuijken 1994; Ostriker & Binney 1989; Rix *et al.* 1992).

If counterrotation arises from accretion of a satellite galaxy, there should be some peculiarity in the environment of these galaxies that may be detectable in the present epoch, as happens in Seyfert or radio-loud galaxies. Possibilities include: 1) a local over-density of galaxies or 2)a larger number of satellites if the accretion event occurred recently. A trace of the satellite accretion may also remain if the phenomenon is not recent; for instance, a deficit of satellites due to depletion of the environment may differentiate them from a normal population. Finally, if the counterrotation is generated by pure gas, pure star infall or by a merger in the early epoch of galaxy formation, no traces of differences should exist in the present surrounding field.

2. Selection of the samples

The first step in this work was to select a sample of galaxies with counterrotation and, as wide as possible, a comparison sample of 'normal' galaxies. The latter should be representative of galaxies without counterrotation but with distributions of luminosity and morphological type similar to that of the galaxies with counterrotation. This selection required a short analysis of the samples.

2.1. Galaxies with counterrotation

Our initial selection from the literature included all known examples of gas or stellar counterrotation. For this selection the compilations of Galletta (1996) and Corsini & Bertola (1998)were used. We removed from the lists a few doubtful examples and those with still unpublished references. These included NGC 2217, with a polar ring seen almost face-on (Bettoni *et al.* 1990) and NGC 4684, with gas streams along a pole-on bar (Bettoni *et al.* 1993) that mimic gas counterrotation. At the end of this selection, our working list contained 49 galaxies, whose names are indicated in the first column of Table 2. They have been divided according to the kind of counterrotation present. Four systems show both kinds of counterrotation and have been considered separately in the statistical analysis. They include IC 4889=IC 4891, NGC 3593, NGC 4550 and NGC 7079. In the following, the label 'gas cr' or 'stars cr' refer only to the pure cases of gas and star counterrotation, while 'all cr' or 'cr galaxies' indicates both samples plus these four galaxies.

The mean astrophysical parameters of these galaxies have been obtained from the Lyon-Meudon Extragalactic Database, (Paturel *et al.* 1997). They are apparent and absolute magnitudes, radial velocity and morphological type.

2.2. Selection of the comparison galaxies

In order to prepare a comparison sample, we made an initial list of galaxies for which both gas and star rotation curves were published. The principal source for this list was the Catalogue of Spatially Resolved Kinematics of Galaxies (Prugniel *et al.* 1998) that is available on the web. The published rotation curves for each galaxy in the list was analysed, in order to determine the data-supported co-rotation for the stars and gas. The comparison sample also includes galaxies studied by Kuijken *et al.* (1996), where the authors claim that no counter-rotating cores have been detected.

This list contains a high percentage of spirals, whereas galaxies with counterrotation mostly have morphological types earlier than Sa. This may alter the comparison between samples, with spiral galaxies generally being present in a lower density environment. To minimize this difference, we extracted from the initial list of comparison galaxies a sub-sample with a distribution of morphological types similar to that of galaxies with counterrotation. This sub-sample was checked to exclude the presence of other biases in their general properties, applying a Kolgomorov-Smirnov test to their distributions of absolute magnitudes M_B, red-shift and morphological type. To this end, we determined the cumulative frequency distribution $S(X)$ for each sample of observations by using the same interval for both distributions. $S(X)$ is the fraction of data observed equal to or less than X. Then, for each interval we subtracted one step function from the other, evaluating D_α=max$|S_1(X) - S_2(X)|$ which is the maximum absolute difference found for the two distributions. The probability of the two samples having the calculated D_α and coming from different galaxy populations is estimated by means of the theoretical significance level SL, which is a function of the sizes of the samples and is tabulated in statisti-

cal books. Comparing various sub-samples of comparison galaxies we found one whose distribution of intrinsic properties is not significantly different, at a confidence level of SL=95%, from that of all the cr galaxies (see Table 1). All the SL values calculated on the basis of the corresponding D_α are lower than this value.

An independent test of the quality of this comparison sample concerns the large scale environment in which these galaxies are located with respect to that of the cr galaxies. We then checked each galaxy for which kind of environment it belongs to: field, small groups and large clusters. This classification was made for galaxies with red-shift $\leq$3000 km s^{-1} by Tully (1987) who indicates for each one the richness and the velocity dispersion of the group to which it belongs. The group richness is also available for galaxies brighter than magnitude 14 and with red-shift lower than 5500 km s^{-1} (Garcia *et al.* 1993).

These data show that the galaxies with counterrotation are present in all kinds of environments, discovered both in clusters as rich as Virgo as well in regions of the sky apparently empty of companions. The distributions of richness and group velocity dispersion show a large spread of values, without any tendency for clustering of data at particular values. As performed for the absolute magnitudes and morphological types, a Kolgomorov-Smirnov test was applied to the samples (see Table 1) and indicates that the differences between galaxies with counterrotations and the comparison sample are not significant.

These tests defined the final list for the comparison galaxies that was used in the following Sections as a reference sample of normal galaxies. It is shown in the first column of Table 3 and contains 43 galaxies.

3. Data production and analysis

To study the properties of the visible environment of these galaxies, we searched all the objects present in the sky around every galaxy, starting from the optical image databases available in the literature. Our research was focused along different lines:

1) a first search of faint objects in the close neighbourhood of each galaxy,

2) a second search of bright objects that may have encountered the galaxy within the last billion years;

3) a comparison of the density of galaxies within 40 Mpc, taken from the literature (Tully 1988), taking into account the presence of the sample galaxies in groups of different hierarchy. This test is an extension of that discussed in Sect. 2.2.

In the following, the galaxy to be studied, located at the centre of each field, will be referred to as the 'central galaxy', whereas all the objects present in the selected field will be called 'nearby objects', even if they are in the foreground or in the background with respect to the central galaxy. Only when the red-shift difference between the nearby object and the central galaxy is lower than a fixed value, described subsequently, will the object be defined as a 'companion'.

3.1. Search for faint objects

The first search was performed by adopting a searching radius of 100 kpc and looking at all the objects present within that radius. The search was performed by extracting the data from the APM Sky Catalogue, available for Internet access from the Observatory of Edinburgh (Irwing *et al.* 1994). It contains data extracted by scanning and photometrically calibrating the B and R plates of the Palomar Sky Survey and the ESO/SRC J survey. It lists all the objects present in the plates over the brightness level of 24 mag arcsec^{-2} for the blue plates and 23 mag arcsec^{-2} for the red plates. They correspond to a limiting apparent magnitude B=21.5 and R=20.0. For each object present in a field corresponding to 100 kpc at the distance of the central galaxy, we extracted the following parameters: α and δ co-ordinates, B and R apparent magnitudes, semi-major axis, ellipticity and P.A. of the ellipse fitting the image. In APM, galaxies are distinguished from stars by means of a comparison of their Point Spread Function with that of an 'average' stellar image.

For most of the objects in the field the true distance is unknown, so we adopted the following method to discard background and foreground objects: all the parameters extracted from APM were converted in distance from the central galaxy (kpc), absolute magnitude and linear size (kpc) *as if* all the objects were at the same distance as the central galaxy. We expected that many background galaxies would appear with a linear size or magnitude too small to be real companions. Similarly, eventual foreground galaxies would appear too big. The limits taken to keep a galaxy were from 2 to 50 kpc for the size and from M_B=-14 to M_B=-23. These figures have been chosen as typical mean size and luminosity of the galaxies, taken from the Local Group members (Zombeck 1990; Sandage & Tamman 1981) and from the Revised Shapley-Ames Catalog (Sandage & Tamman 1981). A limit of this method is given by the fact that galaxies intrinsically fainter than M_B=-14 do exist, e.g. Leo I, whose absolute magnitude is M_B=-9.6 (Sandage & Tamman 1981). It is clear that a more relaxed limit, for instance $M_B \leq$ -9, may include all the possible dwarf galaxies in the surroundings of the central galaxy but will surely fill the sample of nearby objects with a large number of background galaxies. After a set of tests with nearby central galaxies, we chose to limit the sample at M_R=-14, bearing in mind that for fainter limits the possibility of contamination by background objects is higher than the chances of excluding possible dwarfs. Based on the distances of the central object, we computed that an object of M_B=-14 with apparent B magnitudes should always appear brighter than the APM detection limits both for counterrotation and normal galaxy fields. For this reason, we are confident that most of the faint objects around the sample galaxies are present in our search.

A problem to be faced in using the APM data is that the large galaxies present in the field, especially if belonging to late morphological types, appear fragmented in a set

Table 1. Summary of the Kolgomorov-Smirnov tests made to choose a comparison sample of normal galaxies. As explained in the text, D_α is the maximum fractional difference observed between the two distributions, while SL is the significance level at which the two distributions compared are different.

	gas cr vs. no cr		star cr vs. no cr		all cr vs. no cr	
Parameter	D_α	SL	D_α	SL	D_α	SL
Morphological Type	0.344	92.3%	0.220	57.1%	0.240	84.2%
M_B	0.244	60.7%	0.152	13.5%	0.170	44.2%
Red-shift	0.314	86.6%	0.193	40.0%	0.222	77.1%
N. members (Garcia *et al.* 1993)	0.175	<10%	0.157	<10%	0.133	<10%
N. members (Tully 1987)	0.218	22.9%	0.034	<10%	0.118	<10%
Group velocity dispersion (Tully 1987)	0.096	<10%	0.112	<10%	0.058	<10%

of small extended objects, reducing their contribution to the local population of galaxies extracted from APM. For this reason, we had to look at all the fields by plotting the position and size of the objects present around the central galaxies and we compared this map with the image of the same field extracted from Palomar or ESO/SRJ atlases. When a galaxy is not included in the APM catalogue, we extracted its position and size from other catalogues and inserted it in our files. At the end of this correction, our set of data contained 40 galaxies with counterrotation and 38 comparison galaxies, some systems not being present in the APM catalogue. There are 16 galaxies with pure gas counterrotation, whereas 20 systems exhibit pure stellar counterrotation. Four galaxies have both types of counterrotation.

3.2. Search for bright companions

A second search concerned the detection of bright galaxies that may have been gas or star donors during a close encounter. In this case the search area has been defined in a different way: assuming that a companion galaxy exists which may have encountered the central galaxy in the past, its linear distance will be R= ΔV $\cdot$ Δt, ΔV being the relative velocity in space and Δt the time elapsed since the encounter. If we assume a typical maximum value ΔV=600 km s^{-1} and a maximum elapsed time of 1 Gyr, the maximum projected angular distance between the two galaxies seen at a distance d will be R_{max}[arcmin]= 2110.8/d[Mpc], which was our search radius. This corresponds to a linear distance of 0.61 Mpc. We then searched galaxies within a radius of 0.61 Mpc from the central galaxy and having red-shift difference cz lower than 600 km s^{-1} with respect to it.

This time we used the NED database, extracting position, red-shift, apparent magnitude and size of every listed galaxy lying on the sky inside R_{max} and having $\Delta V \leq 600$ km s^{-1} . These data were converted into distances from the central galaxy, differences in radial velocity, absolute magnitudes and linear sizes. In this search, only galaxies with known redshift were included in the sample. The final set of data includes 47 galaxies with counterrotation (18 gas cr, 25 star cr, 4 mixed) and 42 galaxies of the comparison sample. The excluded objects have too wide a field (such as NGC 253, with 14.°6 of search field) or have no published red-shift (e.g NGC 2612).

3.3. Large scale environment

In addition to our data, we also used density values present in the literature and computed on a much wider scale. We extracted from the Nearby Galaxies Catalog (Tully 1988) the values of ρ_{xyz}, the density of galaxies brighter than -16 mag determined within 40 Mpc using a grid of 0.5 Mpc.

To have a direct comparison with our data, a 'galaxy density' from APM and NED data was calculated. In the first case, the total number of observed faint objects within 100 kpc has produced ρ_{APM}, the projected density of faint galaxies in units of Mpc^{-2}. The area of 1 Mpc^2 is merely an arbitrary choice to plot the data and produce large numbers. In the second case, the NED data were used to produce a ρ_{NED}, in galaxies/Mpc^3, corresponding to the mean density of bright objects with known redshift present in a sphere of volume 0.95 Mpc^3, whose radius is the distance covered at a velocity of 600 km s^{-1} in 1 Gyr.

The values so determined from our data are listed in the last columns of Tables 2 and 3 and are plotted in the two panels of Fig. 1 versus ρ_{xyz}.

4. Statistical parameters

The statistical analysis of all fields for the cr galaxies and comparison sample was done defining a set of density parameters for each field:

$$\rho_{ij} = \sum_k r_k^{-i} D_k^j \qquad (1)$$

where r_k is the projected distance between the central galaxy and the kth galaxy, D_k is the projected diameter of the kth galaxy and (i,j) assumes the values 0, 1, (2,2) and (3,2.4). We normalised the D_k and r_k values in units of 100 kpc.

The first three parameters describe the environment of the galaxies with different criteria: the population (ρ_{00}), the total size of sky covered by surrounding galaxies (ρ_{01}), the concentration of surrounding galaxies ρ_{10}. The remaining three are linked with these: ρ_{11} is proportional to the gravitational potential and ρ_{22} to the gravitational

Table 2. Statistical parameters ρ_{ij} and galaxy densities for galaxies with counterrotation

Name	APM data						NED data						galaxy densities		
	ρ_{00}	ρ_{01}	ρ_{10}	ρ_{11}	ρ_{22}	$\rho_{3,2.4}$	ρ_{00}	ρ_{01}	ρ_{10}	ρ_{11}	ρ_{22}	$\rho_{3,2.4}$	ρ_{xyz}	ρ_{NED}	ρ_{APM}
gas cr															
ESO263-G48							1	0.168	0.084	0.014	0.000	0.000		1	
IC 2006							14	1.347	4.680	0.412	0.028	0.014		15	
NGC 128	3	0.264	15.538	1.220	0.568	1.328	10	1.842	17.609	2.354	1.677	5.188		11	100
NGC 253	0	0.000	0.000	0.000	0.000	0.000							0.22		0
NGC 497	5	0.363	6.457	0.483	0.061	0.034	3	0.663	0.580	0.120	0.005	0.001		3	167
NGC 1052	7	0.506	17.999	0.930	0.209	0.273	9	1.408	4.744	0.696	0.123	0.076	0.49	9	234
NGC 1216							2	0.584	2.839	0.857	0.470	0.584		2	
NGC 2768	2	0.147	2.472	0.174	0.015	0.006	2	0.239	0.731	0.076	0.003	0.000	0.31	2	67
NGC 3497	9	0.389	15.892	0.667	0.077	0.059	1	0.142	1.022	0.146	0.021	0.010		1	300
NGC 3626	2	0.080	4.148	0.193	0.028	0.025	10	0.984	5.632	0.518	0.051	0.022	0.32	11	67
NGC 3941	1	0.041	1.650	0.067	0.005	0.002	3	0.374	0.804	0.103	0.004	0.001	0.29	3	34
NGC 4379	3	0.152	4.801	0.263	0.036	0.026	34	2.964	10.198	0.927	0.055	0.014	2.89	36	100
NGC 4546	2	0.071	6.439	0.209	0.023	0.021	2	0.151	0.541	0.042	0.001	0.000	0.27	2	67
NGC 4826	1	0.023	1.299	0.029	0.001	0.000							0.20		34
NGC 5252	5	0.214	7.941	0.358	0.031	0.018	1	0.242	0.272	0.066	0.004	0.001		1	167
NGC 5354	6	0.525	23.129	2.038	1.301	3.848	15	2.801	12.884	2.455	1.076	1.519		16	200
NGC 5898							5	0.788	6.385	0.856	0.252	0.292	0.23	5	
NGC 7007	7	0.241	8.932	0.298	0.013	0.004	0	0.000	0.000	0.000	0.000	0.000	0.14	0	234
NGC 7097	8	0.245	11.739	0.385	0.026	0.014	2	0.197	0.697	0.060	0.002	0.000	0.26	2	267
NGC 7332	3	0.174	11.996	0.629	0.222	0.334	1	0.136	3.310	0.451	0.204	0.304	0.12	1	100
stars cr															
IC 1459	9	0.586	15.543	0.936	0.205	0.186	14	2.033	2.529	0.400	0.026	0.006	0.28	15	300
NGC 936	3	0.199	5.944	0.332	0.042	0.025	5	0.580	3.792	0.439	0.062	0.038	0.24	5	100
NGC 1439							12	1.469	3.114	0.387	0.017	0.003	0.45	13	
NGC 1543	0	0.000	0.000	0.000	0.000	0	11	1.288	1.983	0.211	0.004	0.000	0.95	12	0
NGC 1574	1	0.021	1.828	0.039	0.002	0.001	20	2.376	4.221	0.520	0.022	0.003	0.98	21	34
NGC 1700							0	0.000	0.000	0.000	0.000	0.000		0	
NGC 2841	1	0.021	2.288	0.049	0.002	0.001	3	0.104	1.912	0.062	0.002	0.000	0.13	3	34
NGC 2983							1	0.250	0.215	0.054	0.003	0.000	0.16	1	
NGC 3608	4	0.199	11.118	0.524	0.083	0.087	12	0.988	11.485	1.283	0.534	0.869	0.56	13	134
NGC 4073	9	0.592	12.717	0.805	0.104	0.06	10	1.946	4.652	0.758	0.080	0.031		11	300
NGC 4138	3	0.088	3.942	0.117	0.005	0.002	14	1.494	5.162	0.562	0.043	0.014	0.84	15	100
NGC 4472	6	0.180	11.165	0.345	0.023	0.013	71	4.502	46.441	2.437	0.235	0.283	3.31	75	200
NGC 4477	4	0.213	7.383	0.386	0.053	0.041	39	3.283	13.461	1.222	0.106	0.053	4.06	41	134
NGC 4596	2	0.064	2.632	0.086	0.004	0.002	12	1.574	4.078	0.505	0.041	0.013	2.87	13	67
NGC 4643	0	0.000	0.000	0.000	0.000	0	18	2.700	3.436	0.522	0.030	0.006	0.25	19	0
NGC 4816	6	0.328	9.335	0.528	0.069	0.05	26	4.333	9.467	1.505	0.359	0.464		27	200
NGC 5005	0	0.000	0.000	0.000	0.000	0	8	0.796	1.919	0.210	0.015	0.003	0.28	8	0
NGC 5322	7	0.219	11.397	0.337	0.020	0.011	9	1.344	1.211	0.153	0.003	0.000	0.43	9	234
NGC 5728	6	0.175	8.930	0.287	0.022	0.016	0	0.000	0.000	0.000	0.000	0.000	0.18	0	200
NGC 6684							7	1.137	0.736	0.092	0.002	0.000	0.21	7	
NGC 6701	15	0.549	27.578	0.977	0.082	0.058	0	0.000	0.000	0.000	0.000	0.000		0	500
NGC 7217	0	0.000	0.000	0.000	0.000	0	0	0.000	0.000	0.000	0.000	0.000	0.15	0	0
NGC 7331							3	0.203	1.089	0.066	0.002	0.000	0.33	3	
NGC 7796	6	0.415	10.085	0.718	0.132	0.113	0	0.000	0.000	0.000	0.000	0.000		0	200
UGC 9922A	8	0.287	12.187	0.445	0.029	0.014	1	0.043	4.005	0.174	0.030	0.034		1	267
gas plus stars cr															
IC 4889	10	0.410	16.651	0.680	0.060	0.033	1	0.108	0.315	0.034	0.001	0.000	0.13	1	334
NGC 3593	0	0.000	0.000	0.000	0.000	0	8	1.159	3.301	0.592	0.093	0.036	0.19	8	0
NGC 4550	2	0.080	7.225	0.348	0.095	0.161	7	0.315	7.640	0.396	0.053	0.050	2.97	7	67
NGC 7079	0	0.000	0.000	0.000	0.000	0	1	0.166	0.241	0.040	0.002	0.000	0.19	1	0

Table 3. Statistical parameters ρ_{ij} and galaxy densities for the galaxies of the comparison sample

Name	APM data						NED data						galaxy densities		
	ρ_{00}	ρ_{01}	ρ_{10}	ρ_{11}	ρ_{22}	$\rho_{3,2.4}$	ρ_{00}	ρ_{01}	ρ_{10}	ρ_{11}	ρ_{22}	$\rho_{3,2.4}$	ρ_{xyz}	ρ_{NED}	ρ_{APM}
IC 5063	9	0.267	20.083	0.625	0.055	0.041	2	0.290	0.227	0.037	0.001	0.000		2	300
NGC 488	7	0.380	11.232	0.599	0.056	0.032	3	0.291	2.543	0.200	0.015	0.006	0.28	3	234
NGC 628	0	0.000	0.000	0.000	0.000	0	7	0.553	2.422	0.204	0.012	0.003	0.18	7	0
NGC 1023	2	0.069	2.261	0.078	0.003	0.001	9	0.625	17.799	0.833	0.346	1.328	0.57	9	67
NGC 1275							8	1.754	4.078	0.911	0.156	0.078		8	
NGC 1291	2	0.053	5.320	0.147	0.013	0.01	3	0.270	0.910	0.091	0.004	0.001	0.14	3	67
NGC 1300							4	0.395	1.669	0.187	0.015	0.006	0.71	4	
NGC 1566	2	0.063	3.283	0.104	0.006	0.002	12	2.160	2.320	0.407	0.017	0.002	0.92	13	67
NGC 2613							1	0.124	0.169	0.021	0.000	0.000	0.15	1	
NGC 2787	4	0.121	5.705	0.184	0.012	0.006	3	0.173	0.750	0.038	0.001	0.000	0.06	3	134
NGC 2903	2	0.052	2.081	0.054	0.002	0	0	0.000	0.000	0.000	0.000	0.000	0.12	0	67
NGC 2974	5	0.112	9.964	0.220	0.012	0.007	0	0.000	0.000	0.000	0.000	0.000	0.26	0	167
NGC 3079	3	0.109	6.278	0.251	0.028	0.023	3	0.213	6.280	0.368	0.112	0.207	0.29	3	100
NGC 3190	5	0.263	12.673	0.725	0.159	0.197	12	1.025	12.844	1.642	0.887	1.891	0.52	13	167
NGC 3198	1	0.033	1.078	0.036	0.001	0	1	0.033	0.125	0.004	0.000	0.000	0.15	1	34
NGC 3489	0	0.000	0.000	0.000	0.000	0	11	1.076	2.174	0.219	0.006	0.001	0.39	12	0
NGC 3516	2	0.075	3.821	0.144	0.012	0.007	0	0.000	0.000	0.000	0.000	0.000	0.19	0	67
NGC 3607	6	0.216	22.133	0.806	0.171	0.323	14	0.976	23.177	1.574	0.720	2.310	0.34	15	200
NGC 3623	1	0.142	1.504	0.213	0.045	0.031	7	1.236	4.603	1.055	0.399	0.310	0.44	7	34
NGC 3898	5	0.169	9.638	0.302	0.022	0.015	13	1.145	4.210	0.374	0.038	0.026	0.56	14	167
NGC 3921	20	0.778	32.854	1.393	0.175	0.173	2	0.476	1.976	0.311	0.050	0.027		2	667
NGC 3945	1	0.024	1.546	0.037	0.001	0	4	0.450	1.059	0.090	0.002	0.000	0.50	4	34
NGC 3962	2	0.049	2.826	0.069	0.002	0.001	2	0.211	0.423	0.040	0.001	0.000	0.32	2	67
NGC 4026	1	0.051	1.121	0.057	0.003	0.001	22	2.451	14.406	1.146	0.354	0.833	1.71	23	34
NGC 4027							14	2.139	6.055	0.624	0.044	0.021	0.61	15	
NGC 4036	2	0.051	3.585	0.096	0.006	0.004	5	0.699	1.262	0.163	0.007	0.001	0.44	5	67
NGC 4111	8	0.344	19.254	0.754	0.093	0.08	13	1.138	25.703	1.337	0.340	0.754	1.09	14	267
NGC 4350	1	0.086	3.484	0.300	0.090	0.117	25	2.773	8.731	1.093	0.260	0.328	2.72	26	34
NGC 4379	2	0.111	3.630	0.215	0.034	0.026	34	2.964	10.198	0.927	0.055	0.014	2.89	36	67
NGC 4450	1	0.024	3.509	0.086	0.007	0.006	9	1.083	2.464	0.285	0.012	0.002	1.88	9	34
NGC 4565	5	0.188	6.516	0.251	0.017	0.008	2	0.363	2.851	0.400	0.102	0.101	1.00	2	167
NGC 4579	1	0.029	1.595	0.046	0.002	0.001	35	3.215	8.425	0.849	0.047	0.012	3.26	37	34
NGC 4594	1	0.022	1.543	0.034	0.001	0	2	0.203	0.467	0.044	0.001	0.000	0.32	2	34
NGC 4736	1	0.020	1.020	0.021	0.000	0							0.42		34
NGC 4762	2	0.139	4.719	0.324	0.074	0.071	16	1.534	6.618	0.726	0.131	0.114	2.65	17	67
NGC 5018	5	0.354	7.384	0.491	0.116	0.085	3	0.871	2.590	0.696	0.256	0.250	0.29	3	167
NGC 5055	1	0.045	1.562	0.070	0.005	0.002	4	0.287	1.403	0.067	0.002	0.000	0.40	4	34
NGC 5084	4	0.306	7.022	0.463	0.062	0.038	7	0.950	3.186	0.399	0.035	0.013	0.29	7	134
NGC 5746	4	0.098	5.349	0.132	0.005	0.002	7	0.594	2.978	0.296	0.032	0.014	0.83	7	134
NGC 5846	3	0.457	4.665	0.662	0.261	0.231	14	1.862	28.351	1.264	0.443	2.149	0.84	15	100
NGC 5866	5	0.196	8.878	0.337	0.024	0.012	3	0.513	1.858	0.350	0.077	0.039	0.24	3	167
NGC 6868	7	0.491	14.982	1.007	0.270	0.43	10	1.882	2.565	0.519	0.041	0.008	0.47	11	234
NGC 7052							1	0.161	0.093	0.015	0.000	0.000		1	

force exerted by the surrounding galaxies on the central object, whereas $\rho_{3,2.4}$ is proportional to the tidal interaction between the surrounding galaxies and the central one. The last two parameters amplify the effects present in the parameter ρ_{11}. These parameters were chosen in accordance with similar studies (Heckman *et al.* 1985; Fuentes-Williams & Stocke 1988).

After conversion into linear units, as described in the precedent paragraphs, the diameters and the distances from the central galaxies were converted into units of 100 kpc. The resulting values of the ρ_{ij} for the field of each central galaxy are listed in Table 2 and Table 3. Results from the APM database and NED are presented together in these tables.

After defining the ρ_{ij} parameters for the two samples of counter-rotating galaxies and normal galaxies, a Kolgomorov-Smirnov test was applied to the ρ_{ij} parameters of the local environment (APM data, galaxies within

100 kpc), to that of the intermediate environment (NED, bright galaxies with similar red-shift) and to ρ_{xyz} densities (Tully 1988, on 40 Mpc scale). The results are shown in Table 4.

5. Results

We begins by considering the local densities at three different scales: a close environment within 100 kpc, an intermediate environment inside 0.61 Mpc, defined by a crossing time of 1 Gyr, and a large scale environment inside 40 Mpc. These densities were extracted from the APM, NED and Tully (1988) catalogues respectively. The APM data refers to a projected galaxy density ρ_{APM}, whereas the NED and Tully (1988) data use the red-shift to define 'volume' densities ρ_{NED} and ρ_{xyz} respectively. When these densities are plotted against each other (Fig. 1) we can see that ρ_{xyz}, and ρ_{NED} are correlated. In particular, excluding NGC 4379, all the remaining galaxies with gas counterrotation belong to groups where the density of galaxies $\rho_{xyz} < 0.5$ galaxies Mpc^{-3} and $\rho_{NED} < 1.8$ galaxies Mpc^{-3}. On the contrary, the projected densities extracted from APM data span the entire range of plotted values, without any particular clustering of points. This may be affected by the presence of background objects, which alter the sample, despite our selection criteria defined in Sect. 4, or may suggest that there is no particular clustering of objects in the surrounding of our sample galaxies. However, bearing in mind that our cut-off levels in magnitudes and sizes for possible companion galaxies were quite high, it is more likely that a few satellites were missed rather than having a significant contamination by background objects. We think then that the plot reflects the real situation of the densities existing within 100 kpc of our sample objects.

This segregation/concentration for galaxies with gas counterrotation in Fig. 1 is confirmed by a Kolgomorov–Smirnov test applied to the galaxy densities around the whole sample, except for NGC 4379. The population of galaxies with gas counterrotation and the population of normal galaxies appear to be different at a significance level of 93.7%. However, there is no *a priori* justification for the exclusion of NGC 4379. Its inclusion reduces the significance level to 84% and weakens the difference between populations. The same test applied to the NED and APM densities indicates that the difference between samples decreases when smaller environments are considered (see the last lines of Table 4). We may conclude that, in the limited number of galaxies with pure gas counterrotation available, they tend to lie in less dense groups, on scales larger than ∼0.5 Mpc.

Looking at the other studied parameters, described by the ρ_{ij} quantities (Tables 2 and 3), Kolgomorov-Smirnov tests indicate that no marked differences are evident in APM or in the NED data. In fact, no significance level is above ∼80% (Table 4).

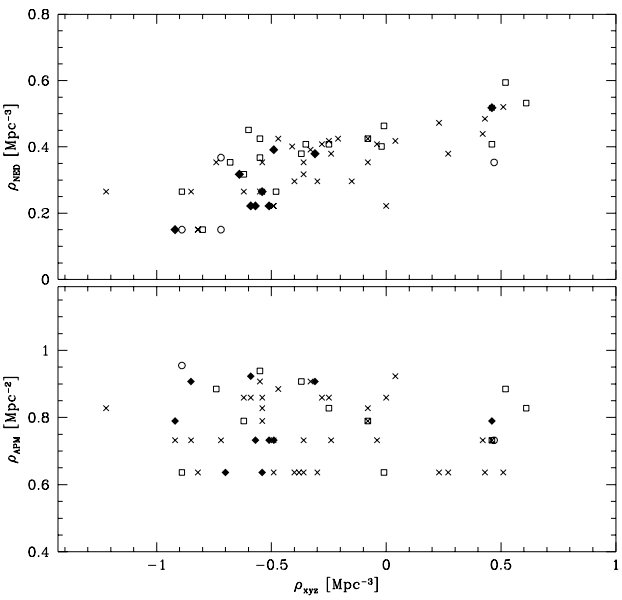

Fig. 1. Plot of the density of objects around all the sample galaxies in environments with different size. The galaxies with pure gas counterrotation or pure stellar counterrotation are indicated by full diamonds and open squares respectively; the normal galaxies are indicated by crosses. The galaxies with both gas and stellar counterrotation are plotted with open circles. *Top panel*: plot of (ρ_{NED}) the density of galaxies/Mpc^3 present in NED database with a crossing time lower than 1 Gyr versus (ρ_{xyz}), the density of galaxies computed within 40 Mpc from Tully (1988). *Bottom panel*: Plot of (ρ_{APM}), the density of galaxies extrapolated to a square of 1 Mpc side on the sky, versus (ρ_{xyz}). These plots are discussed in the text.

6. Conclusions

We deduce that in general the surrounding regions of galaxies with counterrotation do not appear *statistically* different from those of normal galaxies. This result is similar to that found in Paper I for the environment of polar ring galaxies but distinguish our galaxies from the other active galaxy categories (Dahari 1984; Heckman *et al.* 1985; Hintzen *et al.* 1991; Rafanelli *et al.* 1995).

Among the hypotheses presented in the Introduction about the origin of counterrotation and polar rings, our result tend to disprove that of a recent interaction with a small satellite or a galaxy with similar size. If such a process is at the origin of the counterrotation phenomenon (Balcells & Gonzalez 1998; Bekki 1998; Kennicut 1996; Thakar and Ryden 1996), it cannot be younger than 1 Gyr, the crossing time for the volumes of space studied in this paper. Otherwise it is difficult to conceive that no trace of the donor galaxy remains in the surrounding space, both as a single galaxy present in the NED archive or in a form detectable in APM data as diffuse surrounding objects.

Table 4. Summary of Kolgomorov-Smirnov tests on the density parameters calculated from the data extracted from APM and NED databases. D_α is the maximum difference observed between the two distributions, whereas SL is the percentage significance level at which the two distributions compared are different. In the last three lines, we show the results of the tests applied to the density ρ_{xyx} and ρ_{NED} (in galaxies/Mpc^3) and ρ_{APM} (in galaxies/Mpc^2) described in the text.

	gas cr vs. no cr		stars cr vs. no cr		all cr vs. no cr	
Param.	D_α	SL	D_α	SL	D_α	SL
APM (100 kpc environment)						
ρ_{00}	0.178	13.3%	0.292	78.6%	0.217	64.9%
ρ_{01}	0.283	66.9%	0.258	64.9%	0.233	72.9%
ρ_{10}	0.257	54.9%	0.237	54.3%	0.207	58.8%
ρ_{11}	0.207	28.5%	0.179	20.9%	0.179	40.6%
ρ_{22}	0.145	<10 %	0.121	<10 %	0.096	<10 %
$\rho_{3,2.4}$	0.171	10.4%	0.079	<10 %	0.050	<10 %
NED (1 Gyr similar redshift companions)						
ρ_{00}	0.167	12.7%	0.130	<10 %	0.056	<10 %
ρ_{01}	0.206	34.6%	0.242	67.9%	0.166	40.1%
ρ_{10}	0.071	<10 %	0.129	<10 %	0.058	<10 %
ρ_{11}	0.135	<10 %	0.129	<10 %	0.095	<10 %
ρ_{22}	0.111	<10 %	0.150	12.8%	0.097	<10 %
$\rho_{3,2.4}$	0.056	<10 %	0.154	15.4%	0.097	<10 %
densities of galaxies from different catalogues						
ρ_{xyz}	0.372	84.2%	0.140	<10 %	0.238	71.6%
ρ_{NED}	0.206	34.6%	0.155	15.9%	0.063	20.4%
ρ_{APM}	0.178	13.3%	0.203	34.8%	0.153	22.3%

This result, to a first approximation, support the hypothesis that all galaxies are born from a merger process of smaller objects occurring early in their life. However, only a few galaxies that we know of develop counterrotation and polar rings. It may be natural to attribute this peculiarity to a richer environment, which makes the possibility of collisions easier. Our data are also contrary to this hypothesis, because the environment of such galaxies does not appear to be richer in satellites. This is different to Seyfert or radio-loud galaxies which lie in environments with a higher density of companions. On the contrary, if a weak tendency exists for galaxies with gas counterrotation only, it is seen in regions of space where the large scale density of galaxies is smaller. Whatever the special machinery is which produces counterrotation or polar rings instead of a co-planar, co-rotating distribution of gas and stars, it is not connected to the present galaxy density of their environments.

An alternative mechanism to form counterrotation and polar rings may arise from a continuous, non traumatic infall of gas that later formed stars (Voglis *et al.* 1991; Quinn & Binney 1992; Merrifield and Kuijken 1994; Ostriker & Binney 1989; Rix *et al.* 1992). In such a case the past and present visible environment of these galaxies would appear similar to that of the other galaxies, even if the process is still active. This explanation is consistent with all the results we found. The slow infall of matter on a galaxy should not alter either its luminosity distribution or its stellar kinematics, untill the accreted mass is large enough to generate tidal actions. The galaxies with counterrotation and the polar rings may in such a scenario appear relaxed or in equilibrium, even if some star formation is active (see the polar rings of NGC 4650A and NGC 5128).

The study of the peculiar galaxies that present gas accretion is still under discussion of the possible models to explain their origin and evolution. It is currently impossible to decide between the previous, perhaps incompatible, theories (early merging with special dynamical conditions or continuous slow infall). On the other hand, the observations of galaxies with counterrotation, begun in 1984, provide clues to their evolution, but are still not conclusive. To solve the problem, we are planning to study the gas content of galaxies with counterrotation and polar rings (Bettoni *et al.* 2001).

Acknowledgments

We would like to thank Dr. J. Sulentic for useful suggestions regarding this paper. This research was done using the LEDA database,(leda.univ-lyon1.fr), of the NASA/IPAC Extragalactic Database (NED, ned-www.ipac.caltech.edu) which is operated by the Jet Propulsion Laboratory, California Institute of Technology, under contract to the National Aeronautics and Space Administration and of the Hypercat database (www-obs.univ-lyon1.fr/hypercat). This search has been granted by the funds 60%-2000 of the Università di Padova.

References

Balcells, M. & Gonzalez,A.C., 1998, ApJ 505, L109
Barnes, J.E., 1992, ApJ 393, 484
Bekki, K. 1998, ApJ, 499, 635
Bertola, F., Cinzano, P., Corsini,E.M., Pizzella, A., Persic, M.,Salucci, P., 1996, ApJ, 458, L27
Bettoni, D., 1984, The Messenger, 37, 17
Bettoni, D., 1989, AJ, 97, 79
Bettoni, D., Fasano, G., Galletta,G., 1990, AJ, 99, 1789
Bettoni, D., Galletta, G.,Oosterloo, T., 1991, MNRAS, 248, 544
Bettoni, D., Galletta, G., Garcia-Burillo, S., Rodriguez-Franco, A, 2001, AA, submitted.
Bettoni, D., Galletta, G., Sage,L.J., 1999, AA, 280, 121
Bettoni, D. & Garcia-Burillo, S. 1999, in: Galaxy Dynamics: from the Early Universe to the Present, Eds.: F. Combes, G.A. Mamon, and V. Charmandaris, ASP Conference Series, pag. 89
Bender, R., 1988, AA, 202, L5
Brocca, C., Bettoni, D., Galletta, G.,1997, A&A 326, 907 (Paper I)
Caldwell, N., Kirshner, R. P., Richstone, D. O., 1986, ApJ, 305, 136
Ciri, R., Bettoni, D. & Galletta, G., 1995, Nature, 375, 661
Corsini, E. M. & Bertola, F., 1998, Journal of Corean Phys. Soc. 33, 574

Dahari, O., 1984, AJ, 89, 966
Fuentes-Williams, T. & Stocke, J. T., 1988, AJ, 96, 1235
Franx, M. & Illingworth, G. D., 1988, ApJ, 327, L55
Galletta, G., 1987, ApJ, 318, 531
Galletta, G., 1996, in Barred Galaxies, IAU Coll. 117, ed Buta R., Crocker D.A. Elmegreen B.G., ASP Conf. Ser. 91, 429
Garcia A.M., Paturel G., Bottinelli L. & Gouguenheim L., 1993, A & AS, 98, 7
Gunn, J. E. 1979, Active galactic nuclei. (A79-50785 22-90) Cambridge, Cambridge University Press, 1979, p. 213-225.
Heckman, T.M., Carty, T.J., & Bothun, G.D., 1985, ApJ, 288, 122
Hintzen, P., Romanishin, W., Valdes, F., 1991, ApJ, 366, 7
Irwing, M., Maddox, S., Mc Mahon, R., 1994, Spectrum, 2, 14
Jedrzejeswski, R. and Schecther, P. L., 1988, ApJ, 330, L87
Kennicutt, R., 1996 in:New light on galaxy evolution, IAU Symp.171, Ed. Bender, R. and Davies, R. L., p. 11.
Kuijken, K., Fisher, D., & Merrifield, M.R., 1996, MNRAS, 283 543
Merrifield M. R. & Kuijken, K.,1994, ApJ, 432, 575
Ostriker, E.C. & Binney, J. J., 1989, MNRAS, 237 785
Paturel G., Bottinelli L., Di Nella H., Durand N., Garnier R., Gouguenheim L., Lanoix P., Marthinet M.C., Petit C., Rousseau J., Theureau G., Vauglin I., 1997, Astronom. Astrophys. Suppl. Ser. 124, 109
Prada, F., Gutierrez, C.M., Peletier, R.F., & McKeith, C.D. 1996, ApJ 463, L9
Prada, F., & Gutierrez, C.M., 1999, ApJ 517, 123
Prugniel, Ph., Zasov, A., Busarello, G., & Simien, F., 1998, A&AS, 127 117
Quinn, P.J., Hernquist, L., & Fullagar, D.P., 1993, ApJ 403 74
Quinn, T. & Binney, J., 1992, MNRAS 255 729
Rafanelli, P., Violato, M., & Baruffolo, A. 1995, AJ 109 1546
Reshetnikov, V. & Sotnikova, N. 1997, A&A, 325, 933
Rix, H.-W., Franx, M., Fisher, D., & Illingworth, G., 1992 ApJ 400 L5
Rubin, V. C., Graham, J. A., Kenney, J.D. P., 1992, ApJ, 394, L9
Sandage, A. R. & Tamman, G. A., 1981, A revised Shapley-Ames Catalog of Bright Galaxies, Carnegie Inst. of Washington, Washington, D.C.
Thakar, A.R., and Ryden, B.S., 1996, ApJ 461 55
Tremaine, S. & Yu, Q. 2000, MNRAS, 319, 1
Tully, R.B., 1987, ApJ 321 280
Tully, R.B., 1988, Nearby Galaxies Catalog, Cambridge University Press, Cambridge, UK
Voglis, N., Hiotelis, N. & Höfflich, P., 1991, A&A 249 5
Whitmore, B. C., Lucas, R. A., McElroy, D. B., Steiman-Cameron, T. Y., Sackett, P. D. & Olling, R. P. 1990, AJ, 100, 1489
Zombeck, M.,V. 1990, Handbook of Astronomy and Astrophysics, Second Edition (Cambridge,UK: Cambridge University Press).